International Journal on Recent and Innovation Trends in Computing and Communication
ISSN: 2321-8169 Volume: 11 Issue: 9
Article Received: *25 July 2023* ***Revised:*** *12 September 2023* ***Accepted****: 30 September 2023*

LUNG CANCER CLASSIFICATION USING MODIFIED SQUEEZE NET

[1]Nishiya Vijayan, [2]Dr. Jinsa Kuruvilla
[1]Research scholar, APJ Abdul Kalam Technological University, Kerala, India

[2]Assistant Professor, Dept. of ECE,[1,2] Mar Athanasius College of Engineering, Kothamangalam, Kerala, India
Email: [1]p20ecf01@mace.ac.in, [2]jinsak123@gmail.com

Abstract— **Lung cancer is the primary cause of mortality in individuals diagnosed with cancer. Detecting and diagnosing lung cancer early significantly reduces the mortality rate. The early diagnosis of lung cancer is greatly facilitated by medical imaging. The recommendation is to undergo a CT scan, as it has a higher probability of detecting lung cancer during its initial phases. The detection of lung cancer greatly depends on the utilization of advanced deep learning technology, specifically convolutional neural networks, which assist in accurately classifying the CT image. This paper proposed a Modified lightweight SqueezeNet architecture that mixes bottleneck residual network and fully connected layer along with global average pooling in the original network. This modification enhances the classification performance with a slight rise in computational complexity. CT images of 330 patients are used as a data set for testing the proposed technique, which is executed in MATLAB 2022a platform. The proposed method can identify lung cancer and categorize it as either malignant or normal with test Accuracy of 95.76%, Recall-92.94%, Precision of 98.75%, Specificity-98.75%, and AUC-0.9977. The Modified SqueezeNet gives better classification performance against the base SqueezeNet model. The proposed method outperforms traditional deep learning networks like AlexNet, ShuffleNet, ResNet-50, and GoogleNet.**

Keywords- Adam, Deep learning, Lightweight networks, Lung cancer detection, Residual module, SqueezeNet

I. INTRODUCTION

Lung cancer is a serious healthcare issue in India as well as around the world. The American Cancer Society tracks population-based cancer incidence and calculates the number of new cases and deaths each year. According to the report, the number of new cancer cases and cancer-related fatalities in the US is predicted to be around 1.9 million and 609,360, respectively, in 2022. Cancer holds the position of the second highest cause of mortality in the nation, with only heart disease surpassing it in terms of fatality. In India, the number of individuals diagnosed with cancer is expected to increase from 26.7 million in 2021 to 29.8 million by the year 2025. According to a study carried out by the Indian Council for Medical Research, seven particular types of cancer were found to contribute to over 40% of the total disease burden in India. The report also highlights that lung cancer comprises 10.6 % of all cancer cases [1].

The majority of lung cancer patients have the disease for a long time before it is diagnosed. 5-year survival rates range from 70–90% for early diagnosis to 10-15% for late detection. The 5-year survival rate of 70% indicates that 70 out of every 100 lung cancer patients survive for at least five years [2]. This emphasizes the importance of diagnosing cancer in its starting stage to improve survival rates. Patients are screened using low-dose computed tomography scans of the lungs in an effort to identify lung cancer at an early stage. Not everyone benefits from screening, but there are some high-risk individuals for whom it is advantageous. These people range in age from 55 to 78 and have smoked for at least 20 pack-years, are currently smokers, or have recently quit smoking. The mortality rate from lung cancer was reduced by 20% as a result of screening such high-risk individuals [3].

Experienced radiologists must process CT images to identify cancer. Diagnosing lung cancer is a delicate process that takes time and great expertise. Moreover, the variation in interpretation among expert radiologists differs significantly. As a result, computer-aided techniques are needed for accurate diagnosis [4]. The two most commonly used computer-aided approaches are deep neural networks and machine learning-based methods. Deep learning is now being utilized more extensively for computer-assisted diagnosis. Numerous articles have been published to increase the accuracy of computer-aided systems [5].

A significant difficulty in deep learning is the trade-off between classification performance, the need for computational resources, and training times. Efficiency will improve with more layers but at the cost of resources and time [6]. A lighter model with comparable efficiency will effectively optimize resources and time. A deep learning network with fewer parameters and acceptable performance is referred to as a lighter model. Lighter models will perform better in distributed training since they communicate with the servers less often as it has fewer parameters. The network can easily be updated often because lightweight models necessitate less communication.

International Journal on Recent and Innovation Trends in Computing and Communication
ISSN: 2321-8169 Volume: 11 Issue: 9
***Article Received:** 25 July 2023 **Revised:** 12 September 2023 **Accepted**: 30 September 2023*

So, the overhead required when clients export new models can be minimized. The only memory available to Field-Programmable Gate Arrays is on-chip memory, which has a 10 MB capacity. Therefore, when employing CNNs with FPGA, lightweight models could be stored on-chip without any memory constraint. So, this paper considers squeezeNet architecture, a lightweight model with comparable performance to AlexNet but with fewer parameters [7].

II. Literature Review

In the past few years, a variety of different methods like digital image processing [8], Bayesian Classifier [9], Support vector machine [10], k-Nearest Neighbors [11], and Neural network [12] can be applied to the detection and classification of lung cancer diseases. The researchers have started to explore how to identify various diseases from medical images of lung in a quick yet effective way. In recent days, deep-learning algorithms have been popular for the classification of lung cancers from medical images [13]. Deep-layer CNN algorithms are more frequently used for image classification, but due to millions of parameters, the computation becomes highly expensive. The development of lightweight CNN designs enables the implementation of deep neural networks on small devices with minimum computational complexity. SqueezeNet [7], MobileNet [14], and ShuffleNet [15] are some of the lightweight models.

Shukla et al. explained the process of lung cancer detection using 2D SqueezeNet, a lightweight model on the LUNA16 dataset. Pre-processing of the image, data segmentation, data augmentation, model construction, and training of the network layers are the steps involved in the classification process [16].

Michail et al. focused on lowering the computational complexity and runtime necessary for classification systems while keeping high accuracy. The author proposed SqueezeNodule Net, a compact and precise CNN that can efficiently distinguish between cancerous and non-cancerous lung nodules. The compact CNN model serves as the foundation for fire Module-based SqueezeNet, whose design was altered in two distinct manners and evaluated using the dataset LUNA16. SqueezeNodule-Net V1 and V2 each achieve 93.2% and 94.3% accuracy for 2D pictures, respectively. SqueezeNet (3D) used more computing effort and had a 94.3% accuracy compared to SqueezeNodule-Net V2's 95.8% accuracy [17].

In their study, Lakshmanaprabu et al. introduced a comprehensive methodology comprising several stages, namely pre-processing, followed by feature extraction, feature reduction, and finally, classification. Pre-processed images were utilized in order to extract features such as histogram, texture, and wavelet. Before the classification process, dimensionality reduction was carried out using Linear Discriminant Analysis (LDA). The ODNN classifier and MGSA optimization were both used by the classifier. The approach has an accuracy of 94.6% when evaluated against a database of 50 low-dose lung cancer CT images [18].

Joshua et.al proposed an improvised 3D AlexNet with a lightweight design. The proposed approach uses gradient-weighted class activation mapping, which provides visual descriptions to highlight the discriminative regions. On the LUNA 16 dataset, this network achieves 97.17% accuracy using 10-fold cross-validation [19].

In their study, Hongfeng et al. suggested a TransUnet architecture to categorise nodules in lung CT scans. UNet, a transformer component of TransUNet, and a global average pooling layer are present. The transformer network employs global self-attention modeling to encode discriminative characteristics from CT image patches. The lung nodules are located using the UNet architecture. By giving each sample a score, the global average pooling layer categorises the CT images. The suggested network was tested using the LIDC-IDRI dataset, which yielded an accuracy of 84.62%. [21] For classifying lung nodules, Gugulothu et al. created a hybrid deep-learning approach. The recommended approach extracts features using a modified Fish Bee algorithm and segments image using a chaotic bird swarm optimization. The suggested network enhances sensitivity and reduces the frequency of false positives, achieving 96.39% accuracy on the LIDC-IDRI Data Set [20].

Vijayan et.al, implemented a lung nodule classification algorithm using squeeze net with three optimizers. Squeeze net with stochastic gradient descent gives an accuracy of 82.12%, RMSProp optimizer gives an accuracy of 88.12% and adam optimizer gives an accuracy of 90.10% [22].

Biradar et al. proposed a 2D CNN that distinguished between cancerous and non-cancerous lung nodules. One flattened layer, two convolutional, max-pooling and fully connected layers make up the 2D CNN architecture. The model was assessed using data from a Kaggle CT scan dataset. When it comes to recognizing lung nodules, the 2D CNN approach has an accuracy rate of 88.76% [23].

Pang et al. developed a deep neural network-based lung cancer classification utilizing DenseNet, a lightweight network with a dataset from Shandong Provincial Hospital. They also employed an adaptive boost technique to aggregate numerous classification results to improve classification performance. The accuracy of the suggested model was 89.85% [24].

A CNN-LSTM approach is recommended by Mhaske et al. for the precise classification of lung cancer. The steps in the suggested technique are Otsu segmentation, feature extraction by CNN, and classification by RNN-LSTM [25]. Using the LIDC-IDRI dataset, the method's accuracy was assessed, and it scored 97%. The following are this paper's main contributions:
(a) The primary aim of this study is the development of an efficient, lightweight network for the categorization of lung cancer.
(b) A dataset was built using publicly available LIDC data and 500 CT slides from 50 patients that were obtained in DICOM format from a prominent hospital.
(c) The architecture was modified using the residual network to enhance the performance of the basic squeeze net.
(d) It was demonstrated using the generated dataset that the modified squeezeNet architecture and the Adam optimizer produced the best outcomes.
(e) The modified squeezeNet with Adam optimizer

International Journal on Recent and Innovation Trends in Computing and Communication
ISSN: 2321-8169 Volume: 11 Issue: 9
***Article Received:** 25 July 2023 **Revised:** 12 September 2023 **Accepted**: 30 September 2023*

methodology, which was tested against other state-of-the-art methods for classifying lung cancer, achieved the highest accuracy.

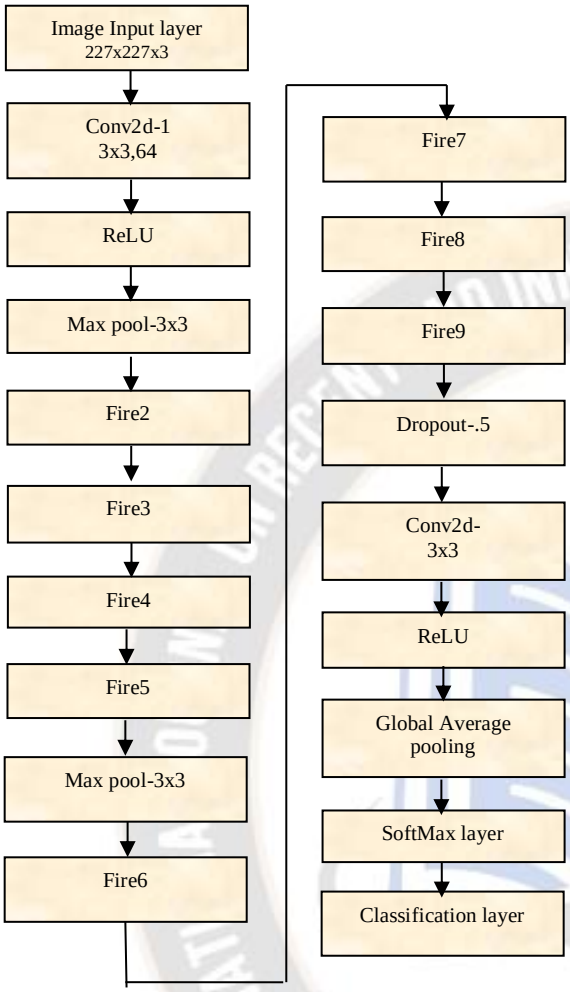

Figure 1. Macro architecture of SqueezeNet

III. Materials and Methodology

A. SqueezeNet

The lightweight network was created to reduce computational complexity and network parameters [7]. While maintaining equivalent accuracy, a smaller CNN architecture will consume fewer resources and can be suited for embedding in memory-restricted devices. So SqueezeNet, a lightweight model, is considered in this research. Researchers from Stanford University, DeepScale, and the University of California, Berkeley designed SqueezeNet in 2016 [7]. SqueezeNet is an eighteen-layer, pre-trained model on Image Net shown in figure 1. The system uses binary classification on a 227 X227 input image as its input.

SqueezeNet is designed to have a compact architecture, about fifty times fewer parameters than AlexNet, and an accuracy comparable to AlexNet. In addition, it requires less communication between servers during training because it is a lightweight network. SqueezeNet can thereby facilitate faster training. The method squeeze net employs to decrease the number of parameters while maintaining accuracy is replacing all traditional 3X3 convolution filters with 1x1 convolution, which results in a nine times parameter reduction.

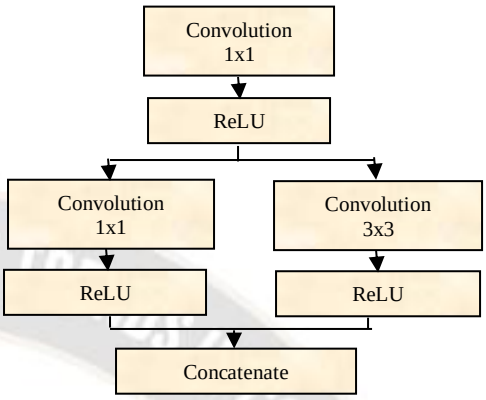

Figure 2. Fire Module

Squeeze layers are used in the second method to limit the number of input channels to 3x3 filters. The above methods focus on reducing parameters while maintaining accuracy. Finally, delayed down sampling is employed in the third method to maintain large activation maps. This will increase accuracy with a constrained set of parameters. The convolution layer, Max pooling, Global average pooling, Relu, Fire Module, Dropout, Softmax, and Classification layer are the different layers in the base squeezeNet model [26][31]. The fire module in Figure 2 represents the fundamental squeezeNet design element. It is made up of an expand layer that mixes 1x1 and 3x3 convolution filters and a squeeze convolution layer that only uses 1x1 filters. One of the Fire Module's three programmable parameters is the number of 1x1convolutional kernels. The number of 1 x 1 and 3 x 3 convolutional kernels in the expand layer are the other two programmable parameters. Compared to the 3x3 and 1x1 kernels in the expand layer, the squeeze layer utilized has fewer convolutional kernels. In other words, the number of inputs to 3x3 filters is decreased by using a 1x1 filter in the squeeze layer. The expand layer enhances the network's ability for representation.

B. Proposed Architecture

In the squeezeNet network, a simple global average pooling method is used to produce the final feature map. But a fully connected layer (FC) could be able to fit better than a pooling layer. An FC is more likely to experience issues with network over-fitting and significant computational overhead. As the FC layer comprises a dense network of neurons, in which each image feature is connected to every other neuron in the FC layer. The complexity of the FC layer is due to the number of parameters. In contrast, a convolutional neural network with a 3x3 filter size only requires nine parameters for each feature map. If the model contains too many parameters, it is more likely to overfit. Due to the huge number of parameters in the FC layer, the model needs to memorize each training sample to account for these additional parameters. This will result in poor performance on test samples, which will overfit the model. Instead of global average pooling in the original network, the

International Journal on Recent and Innovation Trends in Computing and Communication
ISSN: 2321-8169 Volume: 11 Issue: 9
***Article Received:** 25 July 2023 **Revised:** 12 September 2023 **Accepted**: 30 September 2023*

proposed architecture mixes residual network and fully connected layer along with global average pooling. To be more precise, a GAP layer shrinks the feature map to a lower size before sending it to a small FC layer and subsequently to a Softmax and then to the classifier layer.

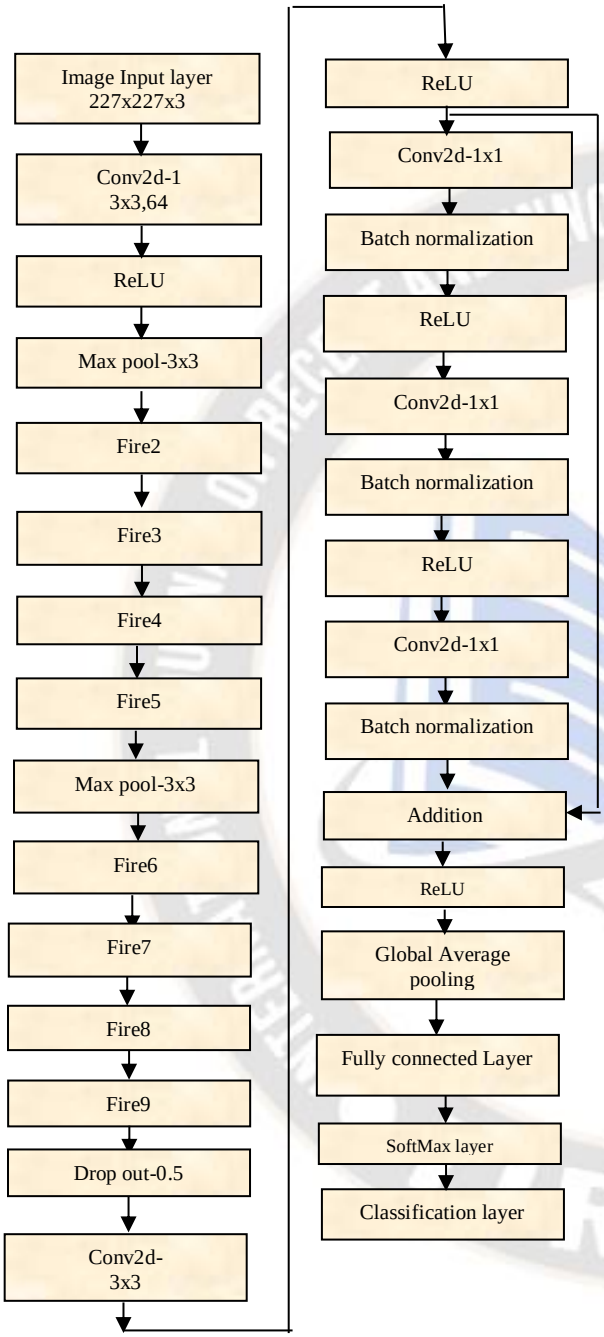

Figure 3: Modified SqueezeNet

Compared to the original network, the modified architecture would enhance the network's ability for fitting, hence enhancing classification performance. The Fully connected layer requires slightly more computational power. With a slight rise in computational complexity, this modification might enhance classification performance. The addition of the fully connected layer may cause overfitting if there aren't enough training data samples. The batch normalization technique is used in the residual network as a solution to this issue. Figure 3 shows the suggested squeezeNet architecture.

The size of the model created using the modified squeeze net architecture is quite small (2.5 MB), allowing it to be implemented for embedded systems, mobile devices, and computational prediction through FPGA servers.

1) Batch Normalization: Normalization refers to the method of transforming the data to have a mean zero and a standard deviation of 1. Each internal layer's input is the previous layer's output. After operations within the preceding layer, the data distribution characteristics will vary, resulting in a changing input distribution for each layer. Consequently, there will be a shift in covariance. When the network is expanding deeper, the covariance shift becomes more, which can be reduced by batch normalization by quickening the convergence of deep networks.

Ioffe and Szegedy introduced batch normalization. After convolution operation, the proposed architecture batch normalization is applied in the last few layers [27]. During training, the variance and mean of the batch data are computed. Then using the previously determined batch statistics, normalize the layer inputs. To retrieve the layer's output, scale and shift it. The batch input from layer M is used in the batch normalization process. The first step is to use equation 1 to calculate the mean of the batch of data. Equation 2 is used to determine the batch's standard deviation. Equation 3 is used to normalize this feature map M.

$$\mu = \sum_{k=1}^{N} \frac{M_k}{N} \quad (1)$$

Where μ is the mean of batch data
N: No. of neurons in the layer
Mk: Design Matrix that contains a mini-batch of the given layer

$$\sigma^2 = \sum_{k=1}^{N} \frac{(M_K - \mu)^2}{N} \quad (2)$$

Where σ - Standard deviation.
In this process, each input is first turned into a mini-batch, and all of the values are then normalized using equations 3.

$$M' = \frac{M_K - \mu}{\sqrt{\sigma^2 + \varphi}} \quad (3)$$

M′: the normalized value
ϕ is a small positive value

$$y_i = \gamma M' + \beta \quad (4)$$

The final step involves applying a linear transformation using equation 4, and the parameters γ and β are learned during training to determine the layer's output, y_i. β enables bias modification, while γ provides for standard deviation adjustment.

Equation 4 guarantees that the inputs have a uniform mean and standard deviation, ensuring that the input distribution to every neuron will be the same. Uniform input distribution will eliminate the covariance shift issue and speed up the convergence of the network.

During test time, the mean and variance are fixed and estimated using the mean and variance previously calculated for each training batch.

2) Residual Network: The neural network's performance was improved by residual networks, which allow skip connections and try to learn different level features. In such a case, the weight will become zero, thus preventing overfitting. It is

International Journal on Recent and Innovation Trends in Computing and Communication
ISSN: 2321-8169 Volume: 11 Issue: 9
***Article Received:** 25 July 2023 **Revised:** 12 September 2023 **Accepted**: 30 September 2023*

challenging to achieve an accurate feature map with just one layer, so adding multiple layers provides more computing power in the form of different levels of convolutions. So, the additional layers don't result in a deeper network. The bottleneck residual architecture is shown in Figure 4, which comprises three convolutional layers. The number of parameters in the residual learning block can be reduced through bottleneck architecture. A 1x1 convolution layer is used first for channel reduction, i.e., it lowers the number of input channels, followed by a 3x3 layer for extracting spatial features and a final 1x1 layer for channel expansion, i.e., it increases the number of input channels to match. With the same number of parameters, the residual network creates a deeper network. With a lightweight squeeze net construction, this network performs effectively [28].

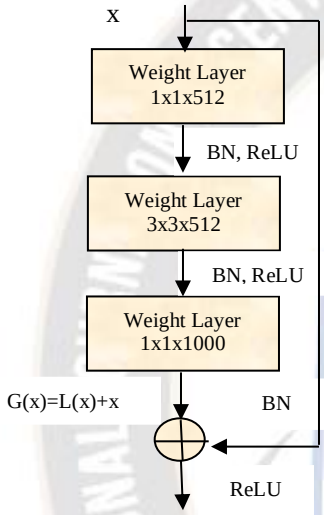

Figure 4. Residual Connection

IV. Experiment Setup and Discussion

A. *Proposed workflow*

The proposed workflow is depicted as a block diagram in figure 5.

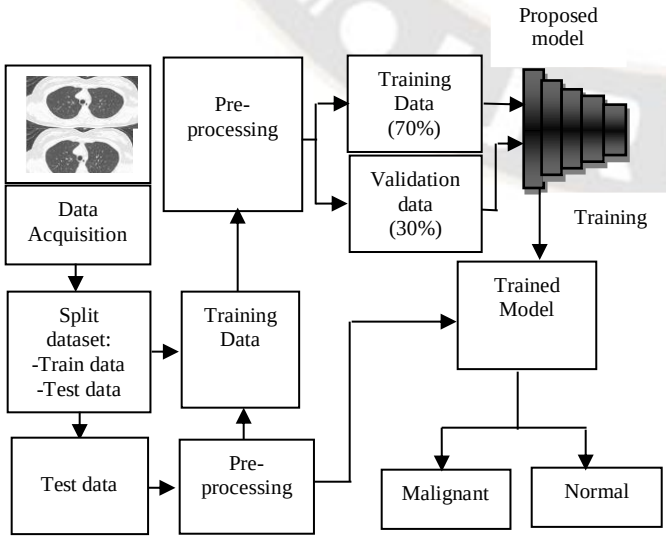

Figure 5. Proposed Workflow

B. *Dataset*

The first step in recognizing lung cancer is forming a database. The images were collected from a renowned hospital with a proper reference from the research institute. The CT image obtained from the hospital database has more than 500 CT slide images from 50 distinct patients in DICOM format with marked nodules by the radiologist. Images were also collected from the LIDC database. 1150 CT slide Images were collected from both LIDC and hospital databases, including both men and women, for training with the help of a radiologist. All the collected images were in DICOM format. A total of 330 images were used for testing, with the remaining set being used to train the model. To prevent over-fitting, validation is applied to 30% of the training data. The LIDC CT scans were referred by two radiologists from separate hospitals, without taking into account the annotations present in the LIDC database. In this work, only malignant and normal cases are considered. The detailed splitting of the dataset is given in table I.

TABLE I. DATASET

Type	Positive	Negative	Total
Train	395	425	820
Test	170	160	330
Total	565	585	1150

C. *Preprocessing*

Pre-processing is done to enhance the cancer nodule visualization within the CT images. In this study, median filtering and adaptive histogram equalization are employed for preprocessing. Median filtering removes noise present in the images while preserving the sharpness of the image. The image's contrast is improved, and the image's edges are highlighted, as a result of adaptive histogram equalization. The preprocessed images are shown in Figure 6.

D. *Online data augmentation*

In the proposed method online augmentation is used. Applying random augmentation to the data will effectively enhance training data. The augmentation makes the networks invariant to distortions in image data. The mini-batches undergo modifications during training through online augmentation. Online augmentation was accelerated on the GPU. RandYReflection function in MATLAB was used to augment the data online, making the network model more robust to lung nodules. In this method, every image from a training set was subjected to a RandYReflection throughout each training epoch.

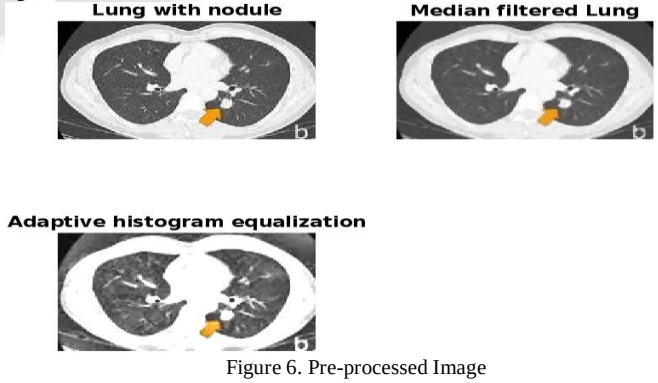

Figure 6. Pre-processed Image

International Journal on Recent and Innovation Trends in Computing and Communication
ISSN: 2321-8169 Volume: 11 Issue: 9
***Article Received:** 25 July 2023 **Revised:** 12 September 2023 **Accepted**: 30 September 2023*

E. Hyperparameter Tuning

Hyperparameters are variables that must be specified before executing a learning algorithm on a dataset. The problem with hyperparameters is that no single unique value fits everything. The optimum numbers depend on the task and the dataset. The hyper-parameters commonly used in deep learning applications are learning rate, Number of epochs, Optimizer, gradient decay factor, Weight initializer, Regularizer, epsilon, and squared gradient decay factor.

F. Adaptive Moment Estimation:

The Adaptive Moment refers to Adam, an adaptable optimization strategy that modifies the learning rate utilizing the Ist and IInd moments. The first and second moments accounted for the average and squared gradients that decreased exponentially which is calculated by equation 5,6. A gradient average with exponential decay improves the performance of the gradient descent process. The updating procedure uses a bias correction technique, selects an adaptive learning rate from RMSprop, and only considers the gradient's smooth form. The computed squared and prior gradients are heavily biased toward zero. The weights are then modified as necessary after computing the first and second moments with bias correction using Equations 7 and 8. Equation 9 shows the updation rule.

$$E[g_{\omega}^2]_N = \beta_2 E[g_{\omega}^2]_O + (1-\beta_2)\left(\frac{\partial loss(\omega_o, b_o)}{\partial \omega_o}\right)^2 \quad (5)$$

$$E[g_{\omega}]_N = \beta_1 E[g_{\omega}]_o + (1-\beta_1)\frac{\partial loss(\omega_o, b_o)}{\partial \omega_o} \quad (6)$$

$$\bar{M}_N = \frac{E[g_{\omega}]_N}{1-[\beta]_l^N} \quad (7)$$

$$\bar{V}_N = \frac{E[g_{\omega}^2]_N}{1-[\beta]_2^N} \quad (8)$$

$$\omega_N = \omega_O - \frac{\eta}{\sqrt{\bar{V}_N}+\varepsilon}\bar{M}_N \quad (9)$$

Where, $E[g_{\omega}^2]_N$]: The first moment, $E[g_{\omega}]_N$ The second moment, β_1 and β_2: Decay rates, $\bar{M}_N$ and $\bar{V}_N$:First and second moments with a bias correction, ω: Network weight, η is the step size or learning rate, and N is the number of iterations

G. Environment

MATLAB 2022a was used as the platform for implementing the lung cancer classification system. The program was run on a 64-bit operating system and an Intel(R) Core (TM) i7-10750H processor running at 2.60 GHz. The system has 16.0 GB of RAM and runs Windows 11 Home Single Language 21H2. It supports a 4 GB NVIDIA GeForce GTX 1650 Ti GPU to improve performance.

H. Training

According to the rule of thumb, the proposed approach separates the dataset into training and testing in a 70:30 ratio when training on the MATLAB platform. Categorical cross-entropy, which acts as the loss function, is calculated using the formula given in Equation 10.

$$Loss = \sum_{l=1}^{L} O_{p,l} \ln P_{p,l} \quad (10)$$

Where l denotes the class label and Pp,l is the anticipated probability observation p for class l. If label l is correctly classified, the binary indicator Op,l has a value of 1; otherwise, it has a value of 0. L is 2 since the classifier is a binary one. The model is trained using ADAM with 400 epochs and a mini-batch size of 64. The model is initialized with the built-in Glorot initializer for all network layers. The other hyperparameters are shown in table II.

TABLE II. HYPERPARAMETERS

Hyperparameter	**Value**
Learning rate	0.0001
Mini batch size	64
No. of Epochs	400
Optimizer	Adam
Weight initialization	Glorot
Epsilon	10^{-9}
Gradient decay actor	0.9
Squared Gradient Decay factor	0.99
Validation frequency	30
Regularization	L_2 Regularizer

V. EVALUATION CRITERIA

An evaluation of the model's performance comprises several metrics. In this paper confusion matrix, accuracy, recall, specificity, precision, and Area Under the ROC curve are used as evaluation parameters [26].

A. Confusion Matrix

A confusion matrix is a complete description of a classifier's performance represented in the form of a matrix. FLPS, FLNS, TRPS, and TRNS are the elements of the confusion matrix. Where, FLPS: False positives, FLNS: False negatives, TRPS: True positives, and TRNS: True negatives, 'PTS' gives the samples that are labelled as positives, NTS' gives the samples labelled as negatives. The confusion matrix for a binary classification problem is shown in table III.

TABLE III. CONFUSION MATRIX

		Predicted		
	Positive	Negative	Total
Actual	TRPS	FLNS	PTS
	FLPS	TRNS	NTS
Total	TRPS+ FLPS	FLNS+TRNS	PTS+NTS

B. Accuracy

When the target variable classes in the data are almost evenly distributed, accuracy is a great measure.

3)Recall

Recall indicates a model's capacity to identify positive samples, regardless of how a negative sample is classified.

C. Precision

Precision provides data about the performance of classifier in terms of false positives. Precision indicates the classifier's ability to correctly categorize all Positive samples and avoid incorrectly classifying a negative sample as Positive.

D. Area under ROC curve

A model's accuracy is evaluated using the area under the ROC curve. The accuracy of the model declines as the area under the curve gets closer to 0.5. A model with perfect accuracy would have an area of 1.

E. Specificity

Specificity represents the TNS rate, and indicates the

International Journal on Recent and Innovation Trends in Computing and Communication
ISSN: 2321-8169 Volume: 11 Issue: 9
Article Received: *25 July 2023* ***Revised:*** *12 September 2023* ***Accepted****: 30 September 2023*

percentage of actual negatives that the model accurately detects. A deep learning classifier with high specificity accurately identifies the majority of the negative cases, whereas one with low specificity may incorrectly label many negative results as positive.

VI. Results and Discussion

In this study, Lung Nodule classification is performed in two different phases. During the first phase, the created dataset was used for evaluating the squeeze net. During the second phase, the proposed architecture was evaluated using the same dataset. The performance of the system is assessed in both cases. First, export the trained model and use it on the test set to determine how well the proposed method work.

Based on the generated confusion matrix, the performance matrix is calculated using the equations specified in section V.

A. Training plot

The following figures, 7 and 8, depict the accuracy and loss of both the original squeezeNet and the modified version during the training and validation processes.

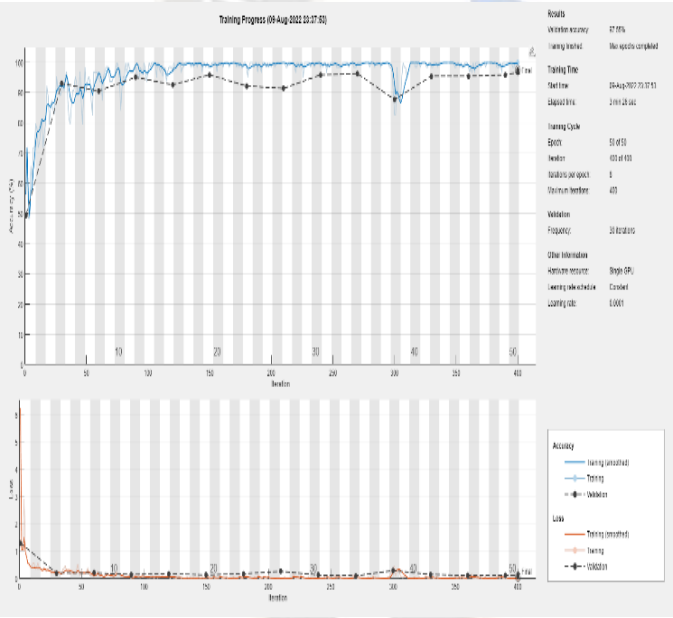

Figure 7. Training Plot- SqueezeNet

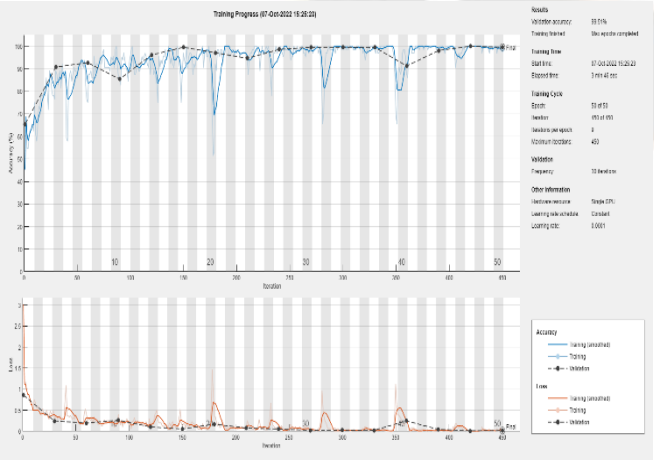

Figure 8. Training Plot- Modified SqueezeNet

B. Confusion matrix

To evaluate how well a classification model is performing, a 2x2 confusion matrix is used, as seen in figure 9,10. This makes it possible for us to fully comprehend how well the suggested classification model works.

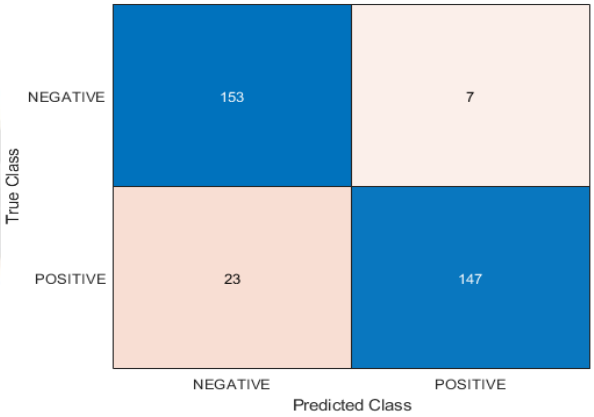

Figure 9. SqueezeNet: Confusion Matrix

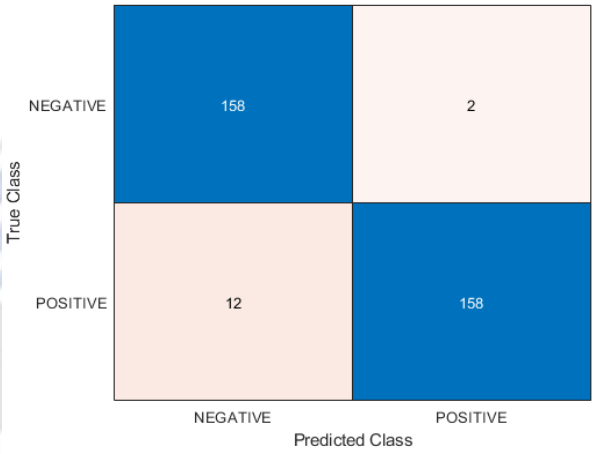

Figure 10. Modified SqueezeNet

C. The Receiver Operator Characteristic (ROC):

The ROC curve can be used as the evaluation tool for binary classification. At various threshold settings, it depicts the TPS rate versus the FPS rate. A classifier's ability to distinguish between two classes is assessed using the area under the curve (AUC). Its value lies between 0 and 1. Its performance is better when close to 1. The ROC curve for squeezeNet and modified SqueezeNet architecture is shown in figures 11,12. The AUC for squeezenet architecture is 0.9755 and for modified squeezenet architecture it is 0.9977.

The table IV presents the accuracy, recall, specificity, and AUC of the proposed method, along with the squeeze net. Modified squeeze nets perform better than squeeze net, as it seen from the table IV.

TABLE IV: Evaluation Metrics

Net	Accuracy	Recall	Precision	Specificity	AUC
Squeeze Net	90.91	86.47	95.45	95.63	0.9755
Modified squeeze Net	95.76	92.94	98.75	98.75	0.9977

International Journal on Recent and Innovation Trends in Computing and Communication
ISSN: 2321-8169 Volume: 11 Issue: 9
Article Received: *25 July 2023* ***Revised:*** *12 September 2023* ***Accepted****: 30 September 2023*

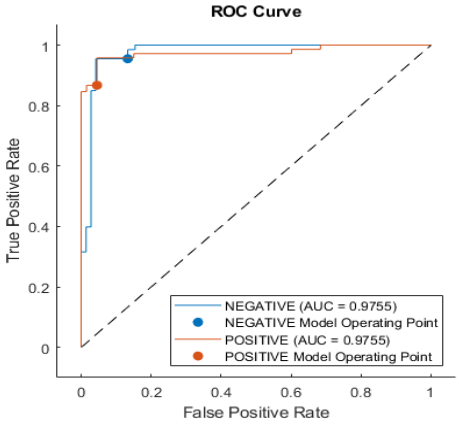

Figure 11. ROC curve-SqueezeNet

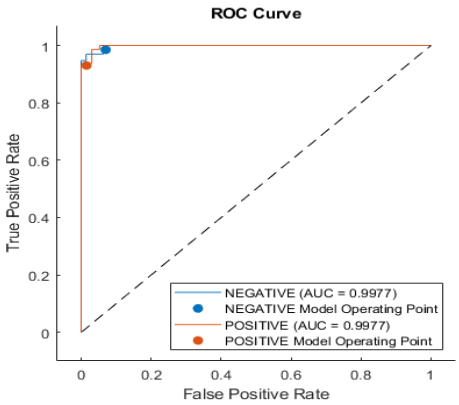

Figure 12. ROC curve - Modified SqueezeNet

D. Comparison with state-of-the art methods

In this section, the suggested method was compared with cutting-edge approaches like ShuffleNet [29], GoogleNet [30], ResNet 50 [30], and AlexNet [31]. Table V shows the parameters, number of layers, and average training time for the suggested method as well as the other present-day methods mentioned above. For better comprehension, the performance comparison is shown as a chart in figure 13. and 14. Figure 13 shows the accuracy, Recall, Precision, and Specificity of SqueezeNet, modified SqueezeNet, ShuffleNet, GoogleNet, ResNet 50, and AlexNet. Figure 14 shows the ROC curve and AUC of SqueezeNet and modified SqueezeNet, with state of art methods for the same dataset. The results indicate that the suggested method works well with our dataset.

TABLE V: COMPARISON WITH STATE – OF - THE-ART NETWORKS

Net	Total learnable Parameters	Average Time (Sec)	No. of Layers
Modified SqueezeNet	2.5M	301	78
SqueezeNet	723.5K	196	68
ShuffleNet	862.8K	460	172
GoogleNet	5.9M	322	144
ResNet 50	23.5M	1227	177
AlexNet	56.8M	277	25

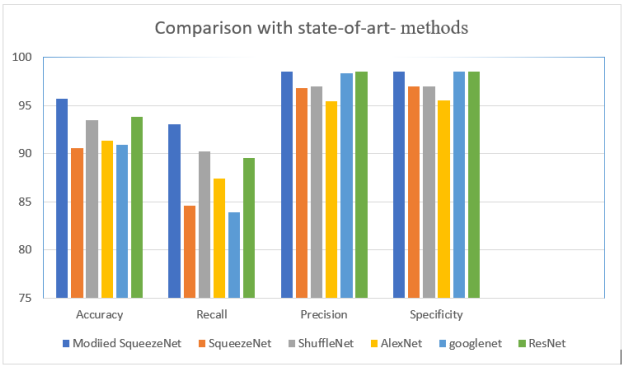

Figure 13. Comparison with State-of-the-art-methods

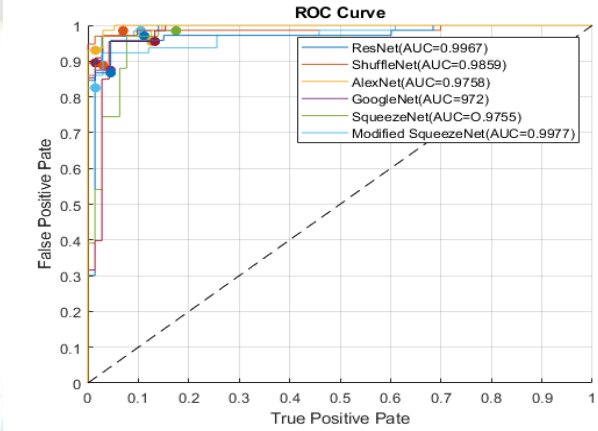

Figure 14.ROC curve- comparison

VII. CONCLUSION

The most prevalent type of cancer in the world is lung malignancy. In recent years, lung cancer has become a serious illness with a poor survival rate. Early identification can significantly reduce the number of fatalities. The convolutional neural network-based deep learning technology is vital in lung cancer detection. The basic concept behind the proposed approach is to classify in a way that provides high performance and cost-effective in terms of calculation. So, in this study, a squeeze net, a lightweight CNN model, was considered instead of a traditional deep learning network. The suggested model has been evaluated on the created dataset and performs noticeably better than SqueezeNet and other conventional models like Alexnet, Shufflenet, ResNet-50, and Googlenet on the same dataset. The proposed method can identify lung cancer and categorize it as either malignant or normal with test Accuracy of 95.76%, Recall-92.94%, Precision -98.75%, Specificity-98.75% and AUC -0.9977. The results were verified by two radiologists from two different hospitals.

FUTURE WORKS

Pre-processing techniques using CNN will be used in the future to improve accuracy. The model can be modified with a vision transformer network. In upcoming work, lung cancer classification can also be done directly using DICOM images.

CONFLICT OF INTEREST

The authors affirm that they have no monetary or other

conflicts of interest.

REFERENCE

[1] Siegel et al., (2022), Cancer statistics, 2022. *CA: A Cancer Journal for Clinicians*, *72*(1), 7–33. https://doi.org/10.3322/caac.21708

[2] Knight et al., (2017), Progress and prospects of early detection in lung cancer. *Open Biology*, *7*(9), 170070. https://doi.org/10.1098/rsob.170070

[3] Kulothungan et al.(2022), Burden of cancers in India - estimates of cancer crude incidence, YLLs, YLDs and DALYs for 2021 and 2025 based on National Cancer Registry Program. *BMC Cancer*, *22*(1). https://doi.org/10.1186/s12885-022-09578-1

[4] Brady, A. P. (2016). Error and discrepancy in radiology: inevitable or avoidable? *Insights Into Imaging*, *8*(1), 171–182. https://doi.org/10.1007/s13244-016-0534-1

[5] Attallah, O., Aslan, M. F., & Sabancı, K. (2022). A framework for lung and colon cancer diagnosis via lightweight deep learning models and transformation methods. *Diagnostics*, *12*(12), 2926. https://doi.org/10.3390/diagnostics12122926

[6] M. Tsivgoulis, Thomas Papastergiou, Vasilis Megalooikonomou (2022), An improved SqueezeNet model for the diagnosis of lung cancer in CT scans. *Machine Learning With Applications*, *10*, 100399. https://doi.org/10.1016/j.mlwa.2022.100399

[7] Iandola et al (2016), "SqueezeNet: AlexNet-level accuracy with 50x fewer parameters and lt;0.5MB model size, arXiv, https://doi.org/10.48550/ARXIV.1602.07360.

[8] Nadkarni, N. S., & Borkar, S. (2019). Detection of Lung Cancer in CT Images using Image Processing. 2019 3rd International Conference on Trends in Electronics and Informatics (ICOEI). https://doi.org/10.1109/icoei.2019.8862577

[9] Dhaware, B. U., & Pise, A. C. (2016), Lung cancer detection using Bayasein classifier and FCM segmentation. International Conference on Automatic Control and Dynamic Optimization Techniques (ICACDOT), 170–174. https://doi.org/10.1109/icacdot.2016.7877572

[10] Sruthi et.al (2022), Cancer Prediction using Machine Learning. 2022 2nd International Conference on Innovative Practices in Technology and Management (ICIPTM). https://doi.org/10.1109/iciptm54933.2022.9754059

[11] Abdullah et.al (2020), Classification of Lung Cancer Stages from CT Scan Images Using Image Processing and k-Nearest Neighbours, *11th IEEE Control and System Graduate Research Colloquium (ICSGRC)*, 68–72. https://doi.org/10.1109/icsgrc49013.2020.9232492

[12] Kuruvilla, J., & Gunavathi, K. (2014), Lung cancer classification using neural networks for CT images. *Computer Methods and Programs in Biomedicine*, *113*(1), 202–209. https://doi.org/10.1016/j.cmpb.2013.10.011

[13] Bouguettaya, A., Kechida, A., & Taberkit, A. M. (2019), A Survey on Lightweight CNN-Based Object Detection Algorithms for Platforms with Limited Computational Resources. *DergiPark (Istanbul University)*. https://dergipark.org.tr/tr/pub/ijiam/issue/52418/654318

[14] Howard et.al (2017), MobileNets: efficient convolutional neural networks for mobile vision applications. *arXiv (Cornell University)*. https://doi.org/10.48550/arxiv.1704.04861

[15] Zhang, X., Zhou, X., Lin, M., & Sun, J. (2017), ShuffleNet: an extremely efficient convolutional neural network for mobile devices. *arXiv (Cornell University)*. https://doi.org/10.48550/arxiv.1707.01083

[16] Shukla et.al, (2021), Lung Nodule Detection through CT Scan Images and DNN Models. *6th International Conference on Inventive Computation Technologies (ICICT), 2021*, 962–967. https://doi.org/10.1109/icict50816.2021.9358545

[17] M. Tsivgoulis, T.Papastergiou, V.Megalooikonomou (2022b), An improved SqueezeNet model for the diagnosis of lung cancer in CT scans. *Machine Learning With Applications*, *10*, 100399. https://doi.org/10.1016/j.mlwa.2022.100399

[18] Lakshmanaprabu et.al, (2019), Optimal deep learning model for classification of lung cancer on CT images. *Future Generation Computer Systems*, *92*, 374–382. https://doi.org/10.1016/j.future.2018.10.009

[19] Joshua, E. S. N. et.al, (2021), 3D CNN with Visual Insights for Early Detection of Lung Cancer Using Gradient-Weighted Class Activation. *Journal of Healthcare Engineering*, *2021*, 1–11. https://doi.org/10.1155/2021/6695518

[20] Wang, H., Zhu, H., & Ding, L. (2022), Accurate classification of lung nodules on CT images using the TransUnet. *Frontiers in Public Health*, *10*. https://doi.org/10.3389/fpubh.2022.1060798

[21] Gugulothu, V. K., & Balaji, S. A. (2023), An early prediction and classification of lung nodule diagnosis on CT images based on hybrid deep learning techniques. *Multimedia Tools and Applications*. https://doi.org/10.1007/s11042-023-15802-2

[23] Vijayan, N., & Kuruvilla, J. (2022b), The impact of transfer learning on lung cancer detection using various deep neural network architectures. *2022 IEEE 19th India Council International Conference (INDICON)*. https://doi.org/10.1109/indicon56171.2022.10040188.

[23] Biradar et.al (2022), Lung Cancer Detection and Classification using 2D Convolutional Neural Network. *2022 IEEE 2nd Mysore Sub Section International Conference (MysuruCon)*, 1–5. https://doi.org/10.1109/mysurucon55714.2022.9972595

[24] Pang, S. et.al , (2020), A deep model for lung cancer type identification by densely connected convolutional networks and adaptive boosting. *IEEE Access*, *8*, 4799–4805. https://doi.org/10.1109/access.2019.2962862

[25] Mhaske, D., Rajeswari, K., & Tekade, R. (2019), Deep Learning Algorithm for Classification and Prediction of Lung Cancer using CT Scan Images. *5th International Conference on Computing, Communication, Control and Automation (ICCUBEA), Pune, India, 2019*, 1–5. https://doi.org/10.1109/iccubea47591.2019.9128479

[26] Vijayan, N., & Kuruvilla, J. (2022), A review on deep learning techniques: Lung cancer classification, CNN Architectures. IJRAR - International Journal of Research and Analytical Reviews (IJRAR), 9(2), E-ISSN 2348-1269, PISSN 2349-5138,. http://ijrar.org/viewfull.php?&p_id=IJRAR22B3053

[27] Ioffe, Sergey, Szegedy, Christian (2015), "Batch Normalization: Accelerating Deep Network Training by Reducing Internal Covariate Shift", arXiv,doi: 10.48550/ARXIV.1502.03167.

[28] Song, X., Chen, K., & Cao, Z. (2020), ResNet-based Image Classification of Railway Shelling Defect. *39th Chinese Control Conference (CCC), 2020*, *6589–6593*. https://doi.org/10.23919/ccc50068.2020.9189112

[29] Gambhir, R., Bhardwaj, S., Kumar, A., & Agarwal, R. (2021), Severity Classification of Diabetic Retinopathy using ShuffleNet. *2021 International Conference on Intelligent Technologies (CONIT)*. https://doi.org/10.1109/conit51480.2021.9498569

[30] Ali et.al (2021), Deep feature selection and decision level fusion for lungs nodule classification. *IEEE Access*, *9*, 18962–18973. https://doi.org/10.1109/access.2021.3054735

[31] Agarwal, A., Patni, K., & Rajeswari, D. (2021). Lung Cancer Detection and Classification Based on Alexnet CNN. *6th International Conference on Communication and Electronics Systems (ICCES), 2021*, 1390–1397. https://doi.org/10.1109/icces51350.2021.9489033